Available online at www.sciencedirect.com

SciVerse ScienceDirect

Ceramics International 38 (2012) 1399–1407

CERAMICS INTERNATIONAL

www.elsevier.com/locate/ceramint

Evaluation of pyroplastic deformation in sanitaryware porcelain bodies

Derya Yeşim Tunçel, Emel Özel *

Anadolu University, Department of Materials Science and Engineering, Eskişehir, Turkey

Received 8 August 2011; received in revised form 6 September 2011; accepted 7 September 2011
Available online 14 September 2011

Abstract

In this study, the effect of composition on the pyroplastic deformation of a sanitaryware porcelain bodies was investigated. Systematic compositional arrangements were made to combine different amounts of SiO_2/Al_2O_3 and Na_2O/K_2O ratios. It was found that fleximeter analyses can be successfully utilised not only to measure the viscosity of a system but also to determine the pyroplastic deformation behaviour of the vitreous bodies. Al_2O_3 and SiO_2 sources affect the mullite formation in the body formulation in that mullite formation increases as the clay–kaolin fraction increases. The composition variation with different Na_2O/K_2O and SiO_2/Al_2O_3 ratios affects the viscosity of the system as the amount of formed mullite increases. The formation of mullite crystals increases the viscosity and diminishes the pyroplastic deformation. In the current study, the formation of about 28 wt% mullite phases with higher viscosity ($\sim 10^{8.34}$ P) values through the combination SiO_2/Al_2O_3:5 and Na_2O/K_2O:4 ratios was sufficient to reduce the pyroplastic deformation of sanitaryware porcelain bodies.

Keywords: D. Porcelain; Pyroplastic deformation; Sanitaryware; Viscosity

1. Introduction

Sanitaryware porcelain is produced from ''vitreous china'' porcelain, which is white and compact, with a water absorption ratio not exceeding 0.5% after firing [1]. These bodies are typically the vitrified product of mixtures of clay, quartz and feldspar after heat treatment at temperatures ranging from 1200 to 1300 °C. Clays give the body the necessary cohesion during drying and plasticity during forming. The quartz is a semi-inert filler material that minimises shrinkage and ensures stability during firing. The flux of feldspar generates the largest part of the essential liquid phase, which allows low-temperature densification or vitrification [2]. The physical properties of sanitaryware porcelain bodies after firing are dependent on a variety of aspects, some of which are the constituent phases relating to high temperature reactions involving the minerals used, the developed microstructures and the degree of densification [3].

The fully vitrified body contains greater than 60 wt% of a glassy phase, which is a viscous liquid at high temperatures and is responsible for undesired shape distortion at high temperatures [2]. There is a tendency toward pyroplastic deformation during the firing of large products such as sinks and closets due to the high amount of glassy phase. Pyroplastic deformation is a distortion of the ceramic shape at high temperatures during firing, and occurs not only because of the flow of this viscous glass at high temperatures, but also because of the applied stress due to the weight of the product during firing.

Many studies on the pyroplastic deformation of porcelains during firing [4–9] have been reported, and considerable correlation between crystal phase formation and the rate of deformation has been established [10]. At the eutectic temperature of 990 °C, quartz dissolution is evident and this process provides silica to the system. A 1150 °C temperature is the point at which the amount of mullite crystals is fixed in the system. Crystal phases also play a key role in pyroplastic deformation. The porcelain system can be thought of as a composite of glassy phase, embedded mullite and residual quartz crystals in the glassy phase. After 1150 °C, system viscosity increases because of mullite formation. In the temperature interval between 990 and 1150 °C, the system has a tendency to form small glass pockets. Because of this tendency, the highest deformation is observed in this temperature interval [10].

The shape and size of crystal phases have effects on the pyroplastic deformation behaviour of porcelain bodies. Porcelain has a heterogeneous microstructure before firing.

* Corresponding author. Tel.: +90 222 3213550x6347; fax: +90 222 3239501.
E-mail address: eozel@anadolu.edu.tr (E. Özel).

0272-8842/$36.00
doi:10.1016/j.ceramint.2011.09.019

Micro-regions of varying composition are present in the unfired ware, including pure clay agglomerates and feldspar-enriched regions. The size and extent of these regions react to form different types of mullite. Mullite crystals derived from pure clay agglomerations are cuboidal and referred as primary mullite. Elongated needle-shaped mullite crystallising from the feldspar-rich melt is termed as secondary mullite. The size and shape of mullite crystals are controlled by the fluidity of the local matrix from which they grow, which depends on the composition and temperature [11]. The development of needle-shaped long mullite crystals in all directions forms three-dimensional interlocking networks, strengthens the porcelain and reduces plastic deformation [4,12].

There is a considerable relationship between pyroplastic deformation behaviour and the grain size, type [13] and chemical composition of raw materials [14]. The fineness of the quartz grains intensifies the dissolution. Pyroplastic deformation increases as dissolution of the quartz in the glass phases takes place and the ratio of the length of the mullite crystals to their diameter decrease [5].

There are also several studies on the effect of composition on the microstructure development and physical properties in porcelain stoneware tiles [8,15,16]. Suvaci and Tamsu [17] reported that the Na_2O/K_2O ratio affects the viscosity of the porcelain stoneware and that as the ratio increases, the viscosity decreases. In addition, the viscosity decrease plays a significant role in microstructure development and the physical properties of porcelain stoneware tiles. Because the crystalline phases and viscosity of liquid phases have critical effects on the microstructure and physical properties of ceramic during firing, these parameters require further and detailed investigation with respect to sanitaryware porcelain to prevent the pyroplastic deformation that arises during firing. Therefore, the research objectives of this study were to determine the effect of the composition design on the viscosity of liquid phases and to evaluate the deformation behaviour of vitreous china bodies by considering the crystalline phases formed in the process.

2. Experimental procedure

In this study, sanitaryware body compositions were prepared by using industrial raw materials. The chemical compositions of these raw materials were determined by X-ray fluorescence (XRF) analyzer (Rigaku, ZSX Primus) (Table 1). A formulation used for industrial production was selected as the standard body composition. Nine different compositions were designed and denoted K1–K9. The Seger formulation approach was applied in order to design new compositions having different combinations of SiO_2/Al_2O_3 and Na_2O/K_2O ratios, and the amount of $SiO_2 + Al_2O_3$ was kept constant in the range of 18.44–23.45 in all compositions. The Seger ratios of the compositions are given in Table 2.

All of the slips were adjusted to have the same physical properties. The solid concentration was held constant at 70% by mass. The liter weight of slips was measured by using a pycnometer and was held at 1770 g/L. The Fordcup viscosity of slips was 55–60 s. However, in the K1 and K2 formulations, the liter weights of slip were adjusted to 1750 g/L due to the higher clay content. The mixture of non-plastic raw materials, namely quartz and feldspar, was ground in a ball mill with alumina balls for 55 min. The particle size distribution of the mixture was measured using a laser particle size analyzer (Malvern, Hydro 2000G). The mean particle size of the mixture, $d_{(50)}$, was kept constant at 12.38 μm for all of the compositions (see Table 3). On the other hand, the particle size distributions of the clays and kaolins were determined by sedimentation analysis (SediGraph 5100) and are given in Table 3.

The samples were shaped using the slip casting method in plaster moulds. To determine the pyroplastic deformation behaviour of compositions, rod-shaped samples having an 85 mm × 7 mm × 7 mm size were produced and fired using an optical fleximeter (Misura, ODLT Flex 1400-30) with a firing regime of 10 °C/min to 650 °C, 5 °C/min to 1000 °C, 3 °C/min to 1250 °C and waiting 40 min at the peak firing temperature. After fleximeter analysis, the pyroplastic index (PI) values of samples were calculated according to Eq. (1) [3]. The viscosity of sanitaryware porcelain bodies (E_p) was calculated using the results of fleximeter analysis according to Eq. (2) [9].

$$\mathrm{PI} = \frac{sb^2}{l^4} \tag{1}$$

$$E_p = \frac{5gl^4\rho_b}{32sb^2} \tag{2}$$

where s is the total deformation, b is the sample thickness, l is the distance between supports, ρ_b is the bulk density of the body, and g is the gravitational constant.

Water absorptions of the samples were measured according to the TST 800 EN 997 standards (Eq. (3)), and the bulk density was determined using the Archimedes principle according to

Table 1
Chemical composition of raw materials.

	SiO_2	Al_2O_3	Fe_2O_3	CaO	MgO	Na_2O	K_2O	TiO_2	LOI
Clay-1	58.30	25.66	1.13	0.16	0.35	0.40	2.24	1.40	10.36
Clay-2	55.14	28.03	2.10	0.24	0.56	0.25	1.59	1.19	10.90
Clay-3	54.58	28.78	1.92	0.43	0.56	0.16	2.32	1.32	9.84
Kaolin-1	47.83	35.75	0.92	0.07	0.46	0.25	2.84	0.00	11.88
Kaolin-2	49.13	35.62	0.87	0.16	0.15	0.13	0.81	0.32	12.77
Sodium feldspar	69.02	18.61	0.25	0.77	0.22	10.18	0.22	0.33	0.40
Quartz	91.45	5.38	0.30	0.03	0.02	0.00	0.31	0.27	2.24

Table 2
Seger formulation of compositions.

Compositions	VC-STD	K1	K2	K3	K4	K5	K6	K7	K8	K9
Na_2O/K_2O	3.92	1.25	3.06	4.81	1.17	3.09	4.90	1.31	3.34	5.21
SiO_2/Al_2O_3	4.68	3.17	3.32	3.43	3.98	4.15	4.15	4.84	4.88	4.84
$SiO_2 + Al_2O_3$	18.44	23.15	23.03	22.78	23.40	22.83	22.78	23.45	23.03	22.80

Table 3
Particle size distribution of raw materials.

Raw materials	Mean particle size (μm)		
	$d_{(10)}$	$d_{(50)}$	$d_{(90)}$
Clay-1	0.18	0.38	7.87
Clay-2	0.18	1.75	13.22
Clay-3	0.18	2.40	19.57
Kaolin-1	0.21	1.55	7.16
Kaolin-2	0.18	0.92	5.34
Mixture of quartz and feldspar	1.74	12.38	40.38

Eq. (4).

$$\%\ \text{Water absorption}\ (w_a) = \frac{w_w - w_d}{w_d} \times 100 \quad (3)$$

$$\text{Bulk density}\ (\rho_b) = \frac{w_d}{w_w - w_s} \times \rho_w \quad (4)$$

where w_w is the wet weight of the sample, w_d is the dry weight of the sample, w_s is the weight of solid suspended in water, and ρ_w is the density of water at room temperature.

The crystalline phases of fired samples were determined using an X-ray diffractometer (XRD, Rigaku Rint 2000) with Cu Kα radiation. Scans were recorded in the 5–70° 2θ range, with a counting time of 10 s per 0.03° 2θ step.

A diffraction/reflectivity analysis program based on the Rietveld method MAUD (Material Analysis Using Diffraction) was used to make quantitative phase analysis. The amounts of glassy phase were obtained by difference, assuming that the bodies contained no other crystalline phases other than mullite and quartz.

The microstructural evolution of the bodies fired at 1250 °C was observed by using scanning electron microscopy with a SEM (EVO-50 VP, Carl-Zeiss, Germany) in combination with energy dispersive X-ray (EDX) spectroscopy (AXS XFlash, Bruker, Germany). The samples were prepared for SEM by automatic polishing. The polished surfaces of samples were chemically etched in aqueous 3% hydrofluoric (HF) acid solution for 10 min.

To investigate the performance of compositions in an industrial manner, specifically shaped large deformation samples were used to measure the amount (in mm) of pyroplastic deformation of selected bodies. The samples for industrial trials were selected according to the lowest pyroplastic index and water absorption values. These samples were fired in an electrical kiln with a firing regime of 10 °C/min to 1000 °C, 5 °C/min to 1250 °C and kept 40 min at the peak firing temperature.

3. Results and discussion

3.1. Effect of chemical and minerological composition on pyroplastic deformation

The chemical and minerological compositions had the primary effects on the deformation at high temperature. For this reason, the crystalline phase compositions of samples fired at 1250 °C were analyzed based on XRD patterns. Because all of the samples had the same kinds of crystalline phases, only the XRD patterns of VC-STD and K6 are given in Fig. 1. Both mullite (JCPDS card no. 15-776) and quartz (JCPDS card no. 46-1045) phases were present in the fired bodies. In addition, the level of glassy phase in the VC-STD sample was found to be slightly higher.

The amounts of crystalline and glassy phases determined by the MAUD method for all of the compositions are given in Table 4. VC-STD consisted of 20 wt% mullite, 20 wt% quartz and 60 wt% glassy phase. The different Na_2O/K_2O and SiO_2/Al_2O_3 ratio combinations affected the phase content of the bodies. The formulated compositions generally contained higher amounts of mullite (ranging from 22 to 40 wt%) and quartz (ranging from 12 to 30 wt%), with a low amount of glassy phase in comparison to the VC-STD composition.

Fig. 2 shows the effect of the Na_2O/K_2O ratio on mullite formation at different SiO_2/Al_2O_3 ratios. Higher amounts of mullite phase were obtained by means of decreasing the SiO_2/Al_2O_3 ratio from 5 to 3. The amount of mullite in the series K1, K2 and K3 having ratios of $SiO_2/Al_2O_3 \cong 3$ and the series K7, K8 and K9 having ratios of $SiO_2/Al_2O_3 \cong 4.8$ slightly decreased with increased Na_2O/K_2O ratios. However, at a $SiO_2/Al_2O_3 \cong 4$ ratio, decreases in the amount of mullite phase in the K4, K5 and K6 series were more distinctive at higher Na_2O/K_2O ratios. These results indicated that the Na_2O/K_2O

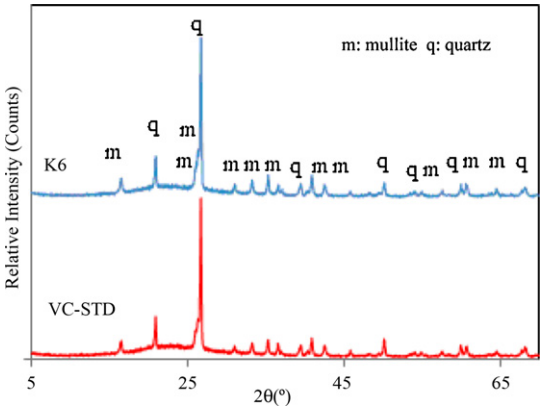

Fig. 1. XRD patterns of samples fired at 1250 °C.

Table 4
Quantitative mineralogical analyses of the sanitary porcelain bodies by MAUD method after firing at 1250 °C (in wt%).

Compositions	VC-STD	K1	K2	K3	K4	K5	K6	K7	K8	K9
Mullite	20	40	35	35	36	31	28	24	24	22
Quartz	20	12	13	16	20	23	24	31	31	30
Glassy phase	60	48	52	49	44	46	48	45	45	48

ratios have a significant role on mullite formation when the ratio of SiO_2/Al_2O_3 is 4. In other words, the amount of K_2O in the formulation affects the mullite formation.

The phase transition sequence and the phase composition while heating kaolinite are intensely affected in the presence of mineralisers such as K_2O, CaO and MgO, which are common crystallographic impurities in kaolinite. In the two-component system, mullite is formed in a molar ratio of $Al_2O_3/SiO_2 \approx 1.5$ above 1400 °C. In a three-component system (and with a larger number of components) containing Na_2O, K_2O, CaO, Fe_2O_3 or TiO_2, the temperature required for mulllite formation is reduced because of the acceleration of reactions due to the presence of a liquid phase, which appears at relatively low temperatures between 950 and 1100 °C [18]. Among these components, K_2O has a distinctive effect on the phase transition of kaolinite [19]. The addition of K_2O to kaolinite as its nitrate has been investigated, and it was found that K_2O accelerated the formation of mullite [20]. In addition, Scroeder and Guertin reported that potash feldspar is the most effective liquid-forming agent for mullite needle growth [21]. Becker et al. [16] also observed that porcelain compositions containing high potash have more mullite than other bodies. This is also important in this study. The amount of mullite decreased with an increase in Na_2O/K_2O, which accounts for the decrease of K_2O in the total alkali fraction (Fig. 2). The reason for the effect of K_2O is probably the higher viscosities of the potassium-rich amorphous phases compared to sodium-containing phases. Higher viscosity liquid phases enhance nucleation, so the growth rate of acicular mullite crystals increases [22].

Mullite formation is also influenced by factors involving the starting raw materials, including the clay–kaolin fraction having a low particle size and a source of thin and reactive SiO_2 and Al_2O_3 for mullite formation [15]. If these conditions are met, the ratio of conversion of mullite increases upon increasing the initial kaolinite content. The SiO_2 and Al_2O_3 content of porcelain bodies can be supplied from the non-plastic raw materials feldspar and quartz sand, or from plastic raw materials like the clay–kaolin fraction. In this work, the amount of SiO_2 and Al_2O_3 provided from kaolinite was increased in the new body formulations. The effect of the amount of Al_2O_3 and SiO_2 provided from kaolinite on mullite formation is presented in Fig. 3. As the amounts of more reactive SiO_2 and Al_2O_3 were increased, the amount of mullite increased. Natural mullite precursors like aluminium silicate minerals are advantageous for the production of mullite because SiO_2 and Al_2O_3 are mixed on a molecular scale into these aluminium silicates [23]. The formation of mullite phase and its distribution betweeen clay and feldspar relicts are controlled by the relative magnitudes of the diffusion rates of the alkali and alumina components and by the contact surface and diffusion distances. As a result, a decrease in particle size of reactants could cause effective diffusion and increases the rate of mullite formation [24].

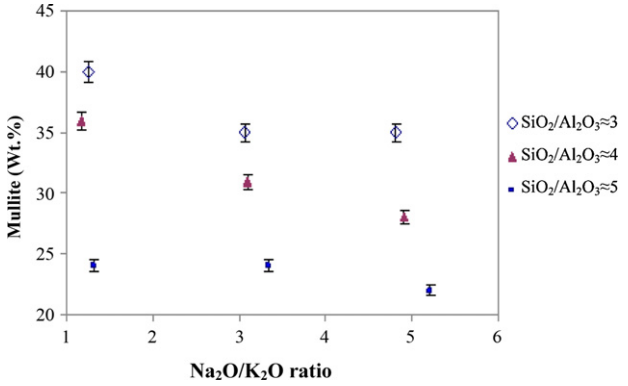

Fig. 2. Effect of the Na_2O/K_2O ratio on the amount of mullite in samples fired at 1250 °C.

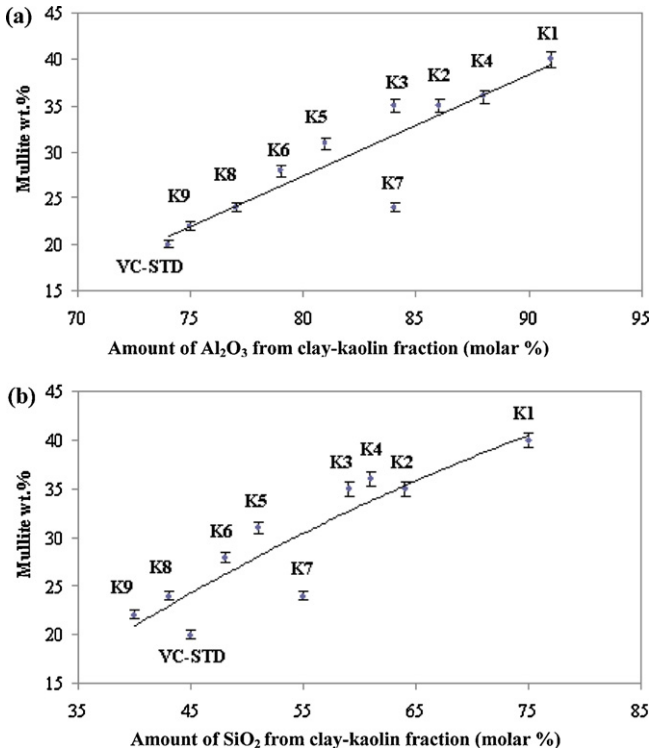

Fig. 3. Effect of (a) Al_2O_3 and (b) SiO_2 provided from kaolin on mullite formation in sanitary porcelain after firing at 1250 °C.

Table 5
The physical properties of fired bodies in fleximeter kiln.

Compositions	Water absorption (wt%)	PI ($\times 10^6$ mm^{-1})	Calculated viscosity (1250 °C) log η (P)
VC-STD	0	2.85	8
K1	0	1.52	8.37
K2	0.22	1.10	8.37
K3	1.41	1.06	8.33
K4	1.11	1.42	8.3
K5	0.79	1.85	8.26
K6	1.52	1.52	8.35
K7	1.88	1.58	8.21
K8	1.47	2.51	7.98
K9	1.41	2.44	8.14

3.2. Effect of viscosity on pyroplastic deformation

Table 5 shows the physical properties of bodies fired in the fleximeter kiln. The VC-STD body and K1 body had 0% water absorption values, whereas other compositions had water absorption values higher than 0.5%, which is concerning for sanitaryware use.

The fleximeter is an optical device that sensitively measures the deformation behaviour of porcelain bodies during firing at the micron level. The magnitude of pyroplastic deformation is determined by the pyroplastic index (PI), which is calculated using Eq. (2). The PI values of compositions are also given in Table 5. Although the K1, K2 and K3 bodies had the lowest PI and water absorption values, rheological problems occurred during shaping of these bodies because of their high clay content of up to 80 wt%. However, K4, K5 and K6 had low PI and water absorption values and good rheological properties. Among the compositions, the K6 body was chosen for detailed investigation and comparison with the VC-STD. The fleximeter curves of the VC-STD and K6 samples are shown in Fig. 4a. The VC-STD body started deformation at a higher temperature (1080 °C) and with higher deformation than the K6 sample (1060 °C).

The deformation rates of samples are also given in Fig. 4b as function of the temperature due to the fact that it results in a better resolution of two or more processes occurring at very close temperatures. Deformation rates in the bodies reach a maximum point at 950 °C, indicating the startup of metakaolin transformation to amorphous free silica, which is the first formed amorphous phase of the system and a spinel-type precursor of the mullite phase [25,26]. At about 1050 °C, feldspars begin to melt and contraction [4] and deformation increases. The early start of deformation of K6 indicated an earlier completion of the formation of liquid phases required for the evolution of mullite crystals at higher temperatures. Metakaolin transformation continues up to 1000 °C and primary mullite is formed from the spinel above 1100 °C [27]. The standard body (VC-STD) deformed rapidly until to the interval 1135–1162 °C. In this temperature region, the deformation rate was somewhat decreased, likely because of the formation of primary mullite crystals. After exceeding that region, deformation continued with an increasing rate up to 1230 °C. It is notable that both of the bodies exhibited the highest deformation rate at 1230 °C. The deformation rate of the K6 body increased and reached a maximum level at 1151 °C. Afterwards, deformation decreased to a level that was close to zero (−0.100), and deformation likely ended at the plateau between 1172 and 1193 °C shown in Fig. 4a. The deformation rate increased again and reached a second maximum at a temperature interval having a midpoint at 1230 °C (Fig. 4b). The rate of deformation increased until 1151 °C, slowed along the mullitisation plateau and again accelerated until 1230 °C. Restrepo and Dinger [4] defined such a region on the linear shrinkage curves of porcelain bodies having different compositions as the ‘‘mullitisation plateau’’. The ‘‘mullitisation plateau’’ is a definite temperature interval in which the rate of shrinkage decreases and the shrinkage curve flattens. In agreement with the literature, the K6 body showed a mullitisation plateau between 1172 and 1193 °C. However, this was not the case for VC-STD; deformation in the VC-STD body occurred at an increasing rate, and there was no delay as in the K6 body (see Fig. 4a). The lower pyroplastic deformation behaviour of the K6 samples could also be correlated with development of the mullitisation plateau during firing.

Conversely, the pyroplastic index values, representative of deformation (1.06–2.51), in new formulated compositions were lower than VC-STD (2.85). The pyroplastic index values of samples generally decrease with an increase in the viscosity of the bulk system. For a particulate suspension such as vitreous china, the bulk viscosity of the particulate–liquid suspension is a more important factor in creep behaviour than the viscosity of the liquid matrix [2]. Increasing temperature causes both an increase in the liquid phase amount and a decrease in the viscosity of the liquid phase [28], but the formation of mullite crystals suppresses the decrease in viscosity.

Therefore, the effect of mullite as a particulate suspension on the bulk viscosity and pyroplastic deformation of the fired bodies was evaluated and the results are shown in Fig. 5. Generally, an increase in mullite content in a fired body caused an increase in the bulk viscosity of the system and a decrease in pyroplastic deformation (see Fig. 5). The K6 body with a higher amount of mullite (28 wt%) strongly resisted deformation compared to VC-STD (20 wt%) with higher viscosity ($10^{8.35}$ P). Consequently, mullite formation plays a key role in pyroplastic deformation reduction by increasing system viscosity, confirming the previous findings of Porte et al. [2],

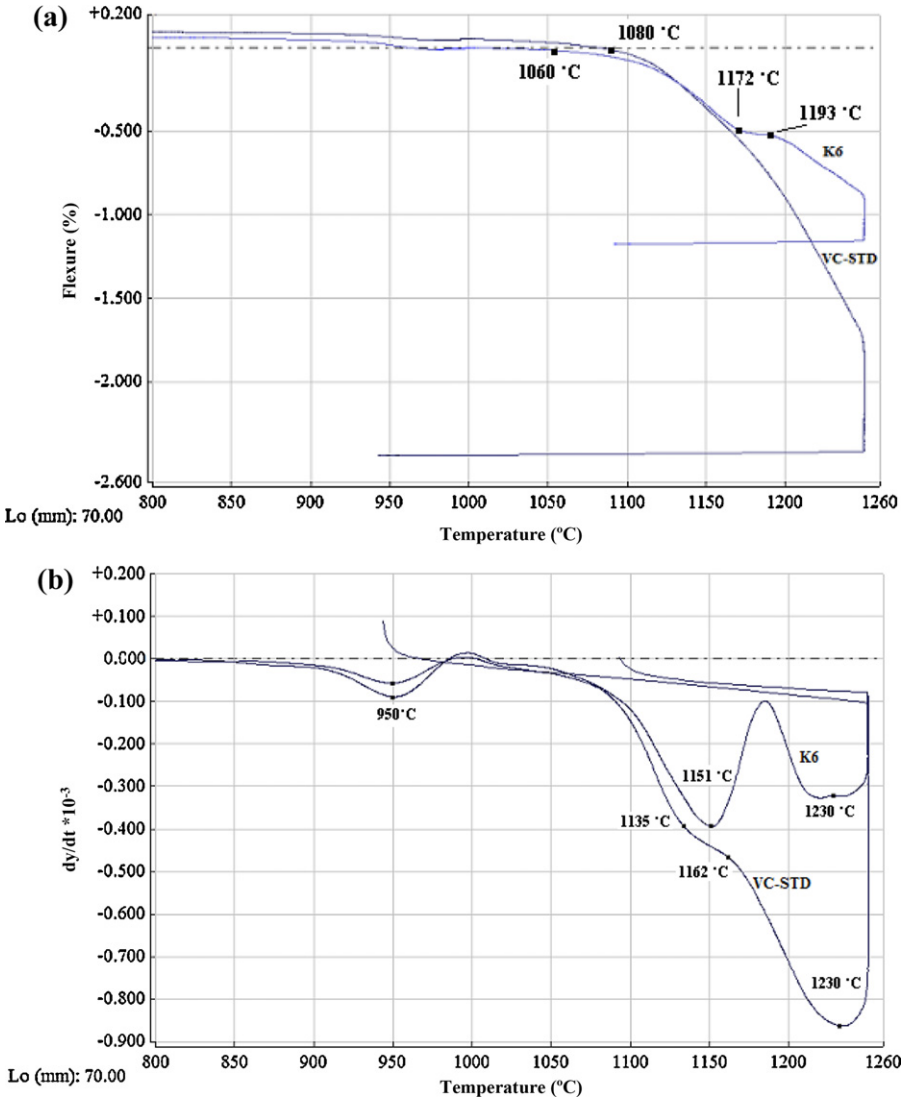

Fig. 4. Deformation behaviour of VC-STD and K6 samples: (a) deformation behaviour of samples and (b) deformation rate of samples.

who reported that particulate phase quartz and mullite crystals control the overall system viscosity and creep behaviour.

3.3. Effect of microstructure on pyroplastic deformation

Two forms of mullite predominate in vitreous systems. Primary mullite is the first to form during firing from the decomposition of "pure" clay and has a cuboidal or scaly morphology. Secondary mullite is the second to form from decomposition of the flux and its reaction with clay, and has a granular or acicular morphology [29]. As alkali diffuses out of feldspar at higher temperatures, secondary mullite nucleates and grows [25]. Because of the fact that X-ray diffraction techniques cannot distinguish between the two types of mullite crystals, scanning electron microscopy has to be used to investigate the distribution of mullite types in the structure. Secondary mullite crystals can only be formed by crystallisation from a melt. The amorphous alumino-silicate formed by reactions between the feldspars and clay minerals provides the necessary liquid [4].

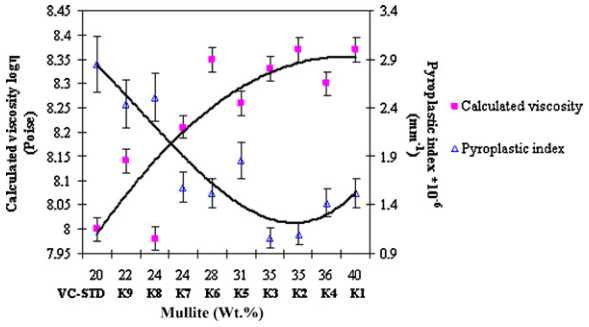

Fig. 5. Effect of amount of mullite on the viscosity and pyroplastic index.

There is a strong relationship between the elimination of pyroplastic deformation and the development of mullite crystals in the microstructure of fired materials [12]. To correlate the pyroplastic deformation with the glassy phases and crystalline phases developed in the microstructure, fired samples were analyzed using SEM-EDX techniques. The microstructural properties of the bodies can be seen in Fig. 6. The K6 body, which had higher viscosity than the standard

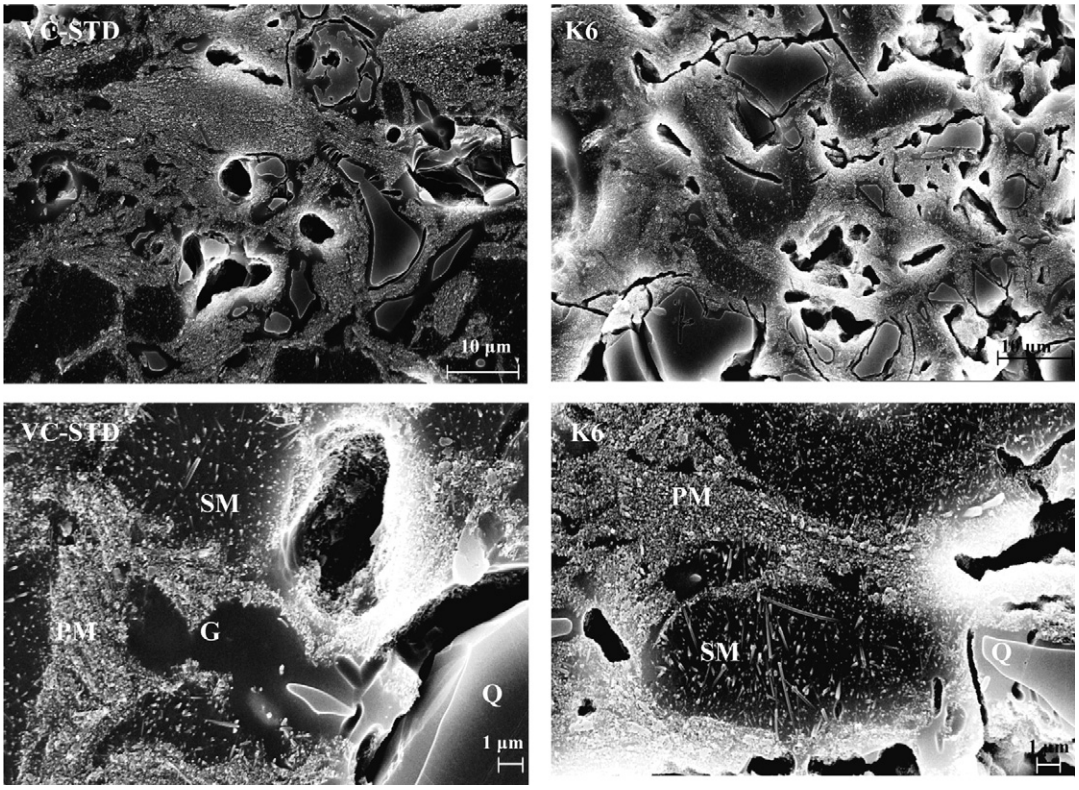

Fig. 6. Microstructure of VC-STD and K6 samples fired at 1250 °C (G: glassy phase; Q: residual quartz; PM: primary mullite; SM: secondary mullite).

body, contained much more, coarser and irregularly shaped porosity than the standard one. This explains the higher water absorption value (1.52) of K6. The constantly dispersed glassy phase of VC-STD inside the microstructure resulted in less porosity and a lower water absorption value (0%).

In both the VC-STD and K6 samples, the crystalline mullite and quartz phases were dispersed in a glassy matrix. The amount of residual quartz in K6 was higher than VC-STD, in accordance with the quantitative phase analysis given in Table 4. At higher magnification, the small primary mullite and coarse needle-like secondary mullite could be distinguished. Feldspar relicts with needle-like secondary mullite crystals and clay relict regions with primary mullite scaly crystals were also observed. Moreover, the K6 body contained a more intensive and continuous distribution of mullite crystals inside the microstructure compared to VC-STD, in accordance with the quantitative phase analysis. Thus, the VC-STD body contained large regions of empty glassy phase due to a lack of mullite crystals. Pyroplastic deformation is the result of low-viscosity glass regions within or surrounding areas of high-viscosity glass and/or crystalline inclusions [6]. Therefore, one of the reasons for the high pyroplastic deformation of VC-STD is the existence of these low-viscosity glass regions within high-viscosity regions containing mullite crystal inclusions. Another reason for the high deformation of VC-STD could be the deficiency of large needle mullite crystals, as shown in the high magnification image of the VC-STD sample (in Fig. 6b). Needle-shaped long mullite crystals randomly oriented in all directions in the microstructure would form a three dimensional network to reinforce the glassy matrix and reduce deforming during glaze firing [4,12].

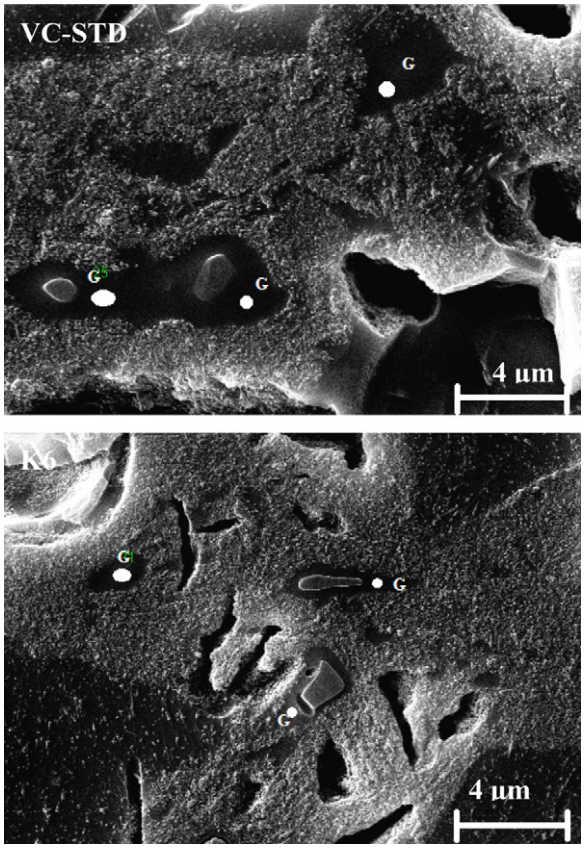

Fig. 7. Glassy regions analyzed by EDX.

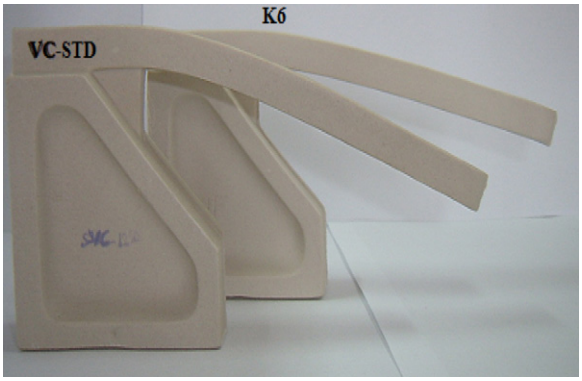

Fig. 8. Industrial test samples after firing in an electrical kiln.

To compare the glassy phase composition of the two samples, EDX analysis was performed from 3 different points (see Fig. 7) for each sample and the average compositions of the glassy phases are given in Table 6. There were significant differences in Al_2O_3 and alkali contents. The glassy phase of the VC-STD body was richer in alkali content ($Na_2O + K_2O$) and Fe_2O_3. For this reason, this alkali-rich glass region reduced the local viscosity and caused more deformation.

3.4. Sample preparation for industrial production

When evaluating the physical and thermal properties of new compositions under industrial firing conditions, only compositions K3, K5, K6 and K7 were tested because they showed promising results in the initial fleximeter analysis. The slips were prepared to have a liter weight of 1795 ± 3 g/L, in accordance with the industrial production standards of the firm. The industrial test samples, which were produced by slip casting in plaster moulds, are presented in Fig. 8. Deformation, after firing in an electrical kiln, was measured as the height difference between the two ends of the samples. The measured deformation in mm and water absorption values of the fired samples are given in Table 7.

The results in Table 7 are consistent with the fleximeter results. The relationship between the pyroplastic deformation values of the compositions were in accordance with the pyroplastic index values, indicating that the fleximeter is a suitable device for testing the deformation behaviour of industrial compositions. In Fig. 8, the K6 sample is shown comparatively with VC-STD. K6 had the lowest water absorption and the pyroplastic deformation value of the K6 composition was 25 mm, 44% lower than that of the standard composition (45 mm). The difference between pyroplastic index values was also similar to the difference between industrial samples.

Table 6
Chemical compositions of glassy phase region shown in Fig. 7.

Oxides	Glassy phase composition (wt%)	
	VC-STD	K6
Al_2O_3	29.51	37.23
SiO_2	62.94	60.08
Na_2O	3.35	0.96
K_2O	1.97	0.95
Fe_2O_3	1.96	0.78

Table 7
The results after firing at electrical kiln and PI values obtained using fleximeter.

Selected compositions	PI ($\times 10^6$ mm^{-1})	Pyroplastic deformation (mm)	Water absorption (wt%)
VC-STD	2.85	45	0
K3	1.06	21	1.27
K5	1.85	27	0.43
K6	1.52	25	0.26
K7	1.58	30	0.46

The difference between the water absorption values between fleximeter rods (Table 5) and industrial samples (Table 7) arose from the difference in liter weights. Slips for fleximeter samples were prepared to have a lower liter weight to provide slip casting for the compositions with high clay contents. The higher liter weight of industrial samples causes a good green packing, thereby lowering the porosity content, leading to a lower water absorption after firing.

4. Conclusions

In this study, it was found that fleximeter analyses can be successfully utilised to measure the viscosity of systems and determine the pyroplastic deformation behaviour of vitreous bodies. The correlation between the deformation behaviour of fleximeter rods and large industrial samples provides confidence in using fleximeter analysis for further industrial composition research. Al_2O_3 and SiO_2 sources affect mullite formation as the clay–kaolin fraction increases, with mullite formation concurrently increasing. In addition, it was found that the composition variation with different Na_2O/K_2O and SiO_2/Al_2O_3 ratios affects the viscosity of the system as the amount of formed mullite increases. The formation of mullite crystals increases the viscosity and diminishes pyroplastic deformation. In the current study, the formation of about 28 wt% mullite phases was sufficient to reduce pyroplastic deformation. In conclusion, if the body composition is prepared with a SiO_2/Al_2O_3:5 and Na_2O/K_2O:4 ratio, large and flat vitreous bodies with low water absorption can be produced with low pyroplastic deformation.

Acknowledgements

The authors would like to thank the Industrial Ph.D. Programme of the State Planning Organisation of Turkey (Project No.: 2004K120270). Special thanks also go to the authorities and people of Duravit A.Ş. of Turkey, who assisted in carrying out this study.

References

[1] D. Fortuna, Sanitaryware, Gruppo Editoriale Faenza Editrice S.P.A., 2000 pp. 55–61.
[2] F. Porte, R. Brydson, R. Rand, R. Riley, Creep viscosity of vitreous china, Journal of American Ceramic Society 87 (5) (2004) 923–928.

[3] A. Pagani, F. Francescon, A. Pavese, V. Dilla, Sanitary-ware vitreous body characterization method by optical microscopy, elemental maps, image processing and X-ray powder diffraction, Journal of the European Ceramic Society 30 (6) (2010) 1267–1275.
[4] J.J. Restrepo, D.R. Dinger, Control of pyroplastic deformation in triaxial porcelain bodies using thermal dilatometry, Interceram 44 (6) (1995) 391–398.
[5] S.M. Olhero, G. Tari, J.M.F. Ferreira, Feedstock formulations for direct consolidation of porcelains with polysaccharides, Journal of the American Ceramic Society 84 (4) (2001) 719.
[6] W.M. Carty, Observations on the glass phase composition in porcelains, Ceramic Engineering and Science Proceedings 23 (2) (2002) 79–93.
[7] A.M. Bernardin, D.S. Medeiros, H.G. Riella, Pyroplasticity in porcelain tiles, Materials Science and Engineering A 427 (2006) 316–319.
[8] E. Rambaldi, W.M. Carty, A. Tucci, L. Esposito, Using waste glass as a partial flux substitution and pyroplastic deformation of porcelain stoneware tile body, Ceramics International 33 (2007) 727–733.
[9] M. Raimando, C. Zanelli, G. Guarini, M. Dondi, R. Fabbroni, T. Cortesi, Process of pyroplastic shaping for special-purpose porcelain stoneware tiles, Ceramics International 35 (5) (2009) 1975–1984.
[10] M.D. Noirot, W.M. Carty, Dynamic pyroplastic deformation study: digital time-lapse photography of porcelain firing, Ceramic Engineering and Science Proceedings 24 (2) (2003) 133–147.
[11] W.E. Lee, Y. Iqbal, Influence of mixing on mullite formation in porcelain, Journal of the European Ceramic Society 21 (14) (2001) 2583–2586.
[12] A. Capoglu, A novel low-clay translucent whiteware based on anorthite, Journal of the European Ceramic Society 31 (2011) 321–329.
[13] N.K. Mitra, A. Basumajumdar, S.K. Das, S. Saha, et al., Development of zirconia porcelain in presence of active silica and its characterization, Journal of the Indian Chemical Society 8 (6) (2004) 531–533.
[14] S.K. Das, K. Dana, Differences in densification behaviour of K-and Na-feldspar containing porcelain bodies, Thermochimica Acta 406 (2003) 199–206.
[15] A. De Noni Jr., D. Hotza, V.C. Soler, E.S. Vilches, Influence of composition on mechanical behaviour of porcelain tile. Part I. Microstructural characterization and developed phases after firing, Material Science and Engineering A 527 (2010) 1730–1735.
[16] C.R. Becker, S.T. Misture, W.M. Carty, The role of flux choice in triaxial whiteware bodies, Ceramic Engineering and Science Proceedings 2 (2000) 1–2.
[17] E. Suvaci, N. Tamsu, The role of viscosity on microstructure development and stain resistance in porcelain stoneware tiles, Journal of the European Ceramic Society 30 (15) (2010) 3071–3077.
[18] D.V. Andreev, A.I. Zakharov, Ceramic item deformation during firing: effects of composition and microstructure, Refractories and Industrial Ceramics 50 (4) (2009) 298–303 (Review).
[19] H. Lin, J. Li, J. Wu, Effects of different potassium salts on the formation of mullite as the only crystal phase in kaolinite, Journal of the European Ceramic Society 29 (2009) 2929–2936.
[20] S.M. Johnson, J.A. Pask, J.S. Moya, Influence of impurities on high-temperature reactions of kaolinite, Journal of American Ceramic Society 65 (1982) 31–35.
[21] J.E. Schroeder, J.P. Guertin, Extremely High Strength Porcelain, McGraw-Edison Company, Franksville, WI, 1978(Research Project), p. 722.
[22] W.D. Kingery, H.K. Bowen, D.R. Uhlmann, Introduction to Ceramics, John Wiley & Sons, New York, NY, 1976.
[23] S.C. Vieira, A.S. Ramos, M.T. Vieira, Mullitization kinetics from silica- and alumina-rich wastes, Ceramics International 33 (2007) 59–66.
[24] S.T. Lundin, Microstructure of Porcelain, vol. 257, National Bureau of Standards Miscellaneous Publication, 1964, pp. 93–103.
[25] W.M. Carty, U. Senapati, Porcelain-raw materials, processing, phase evolution and mechanical behaviour, Journal of American Ceramic Society 81 (1) (1998) 3–20.
[26] L. Carbajal, F. Rubio-Marcos, M.A. Bengochea, J.F. Fernandez, Properties related phase evolution in porcelain ceramics, Journal of the European Ceramic Society 27 (2007) 4065–4069.
[27] K. Dana, S. Kumar Das, Evolution of microstructure in flyash-containing porcelain body on heating at different temperatures, Bulletin of Materials Science 27 (2) (2004) 183–188.
[28] J. Martin-Marquez, J.Ma. Rincon, M. Romero, Mullite development on firing in porcelain stoneware bodies, Journal of the European Ceramic Society 30 (2010) 1599–1607.
[29] W.M. Lee, D.D. Jayaseelan, S. Zhang, Solid–liquid interactions: the key to microstructural evolution in ceramics, Journal of the European Ceramic Society 28 (2008) 1517–1525.